



# OPEN Metabolomic profile of severe COVID-19 and a signature predictive of progression towards severe disease status: a prospective cohort study (METCOVID)

Roger Mallol<sup>2,7</sup>, Alexander Rombauts<sup>3,7</sup>✉, Gabriela Abelenda-Alonso<sup>3,5</sup>, Carlota Gudíol<sup>3,4,5,6</sup>, Marc Balsalobre<sup>1</sup> & Jordi Carratalà<sup>3,4,5</sup>

Profound metabolomic alterations occur during COVID-19. Early identification of the subset of hospitalised COVID-19 patients at risk of developing severe disease is critical for optimal resource utilization and prompt treatment. This work explores the metabolomic profile of hospitalised adult COVID-19 patients with severe disease, and establishes a predictive signature for disease progression. Within 48 hours of admission, serum samples were collected from 148 hospitalised patients for nuclear magnetic resonance (NMR) spectroscopy. Lipoprotein profiling was performed using the <sup>1</sup>H-NMR-based Liposcale test, while low molecular weight metabolites were analysed using one-dimensional Carr-Purcell-Meiboom-Gill pulse spectroscopy and an adaptation of the Dolphin method for lipophilic extracts. Severe COVID-19, per WHO's Clinical Progression Scale, was characterized by altered lipoprotein distribution, elevated signals of glyc-A and glyc-B, a shift towards a catabolic state with elevated levels of branched-chain amino acids, and accumulation of ketone bodies. Furthermore, COVID-19 patients initially presenting with moderate disease but progressing to severe stages exhibited a distinct metabolic signature. Our multivariate model demonstrated a cross-validated AUC of 0.82 and 72% predictive accuracy for severity progression. NMR spectroscopy-based metabolomic profiling enables the identification of moderate COVID-19 patients at risk of disease progression, aiding in resource allocation and early intervention.

**Keywords** SARS-CoV-2, COVID-19, Prognosis, Severity, Metabolomics, NMR, Spectroscopy

The clinical manifestations of SARS-CoV-2 infections vary widely, ranging from an asymptomatic state to severe pneumonia, including acute respiratory distress syndrome (ARDS), multisystem organ failure, and eventually death<sup>1,2</sup>. Morbidity and mortality are almost exclusively driven by the development of ARDS. Certain genomic regions<sup>3</sup>, ACE2 polymorphism<sup>4</sup>, immunological imprinting due to prior infections with other coronavirus<sup>5</sup> and an excessive proinflammatory immune dysregulation play a role in coronavirus disease 2019 (COVID-19) outcomes<sup>6–8</sup>.

Patients hospitalised with COVID-19 remain at a high risk of mortality, ranging from 5 to 15% during delta and late omicron periods<sup>9</sup>. Early identification of the subset of hospitalised COVID-19 patients who will develop severe disease is critical for adequate resource allocation and prompt initiation of treatment. Clinical predictors of severity such as male sex, older age, hypertension and a higher number of comorbidities were rapidly identified<sup>10,11</sup>; nevertheless, it remains unclear why some hospitalised, a priori low-risk patients develop severe pneumonia with ARDS and why others with several risk factors present a favourable evolution.

<sup>1</sup>Human Environment Research, La Salle-Universitat Ramon Llull, 08022 Barcelona, Spain. <sup>2</sup>Fundació Institut Universitari per a la recerca a l'Atenció Primària de Salut Jordi Gol i Gurina (IDIAPJGol), 08007 Barcelona, Spain.

<sup>3</sup>Department of Infectious Diseases, Hospital Universitari de Bellvitge-IDIBELL, 08907 Barcelona, Spain.

<sup>4</sup>Department of Medicine, Universitat de Barcelona, 08007 Barcelona, Spain. <sup>5</sup>Centro de Investigación Biomédica en Red de Enfermedades Infecciosas (CIBERINFEC), Instituto de Salud Carlos III, 28029 Madrid, Spain. <sup>6</sup>Institut Català d'Oncologia (ICO), Hospital Duran i Reynals, 08908, Barcelona, Spain. <sup>7</sup>Roger Mallol and Alexander Rombauts contributed equally to this work. ✉email: alexander.rombauts@gmail.com

Several studies have investigated the underlying metabolic alterations associated with COVID-19,<sup>12–27</sup> most with an emphasis on discriminating between SARS-CoV-2 infected patients from non-infected individuals. Notable alterations have been observed among SARS-CoV-2 infected patients, including glycerophospholipid metabolism remodeling<sup>12–14</sup>, enriched purine metabolism<sup>12,16</sup>, lipoprotein distribution changes marked by elevated VLDL and triglycerides<sup>17,18,28</sup>, and dysregulation in glycolysis<sup>28</sup>. Moreover, increased COVID-19 severity has been associated with disruptions in mitochondrial activity<sup>17,20,21</sup>, altered fatty acid oxidation<sup>20</sup>, reduced amino-acids reflecting a catabolic state<sup>17,21–23</sup>, impaired cholesterol homeostasis<sup>12,14,17,24</sup> and a decline in tryptophan reflecting immune dysregulation<sup>25–27</sup>. Additionally, low levels of circulating lysoPCs and PCs have been directly associated with COVID-19 severity<sup>12,20,23,26</sup>.

Few studies have aimed to identify a metabolomic signature capable of predicting COVID-19 progression<sup>13,25,26</sup>. Most of the patients included in these studies had already progressed to critical states when their blood samples were collected, and the metabolomic profile correlated with COVID-19 severity rather than with the risk of disease progression. Nuclear magnetic resonance (NMR) spectroscopy stands out among the possible metabolomics analytical platforms due to its rapid, highly accurate, non-destructive, and quantitative features<sup>29,30</sup>. To our knowledge, however, only one NMR-based study, involving a cohort of only 36 patients, has explored a prognostic metabolomic profile for mortality<sup>31</sup>.

In this study, we aimed to define the metabolomic profile of hospitalised adult COVID-19 patients who progressed to severe disease using NMR spectroscopy and to establish a predictive signature for assessing the risk of disease progression.

## Results

### Cohort characteristics

The clinical characteristics, blood test results at the time of sampling, COVID-19 treatment and outcomes of the 148 hospitalised COVID-19 patients included are summarized in Tables 1 and 2. Patients were classified according to the WHO Clinical Progression Scale at baseline and over the course of their hospitalisation. One hundred and twenty-six (85.1%) patients had moderate disease status (categories 4 and 5) at baseline of whom 19 (12.8%) progressed to severity and 108 (72.3%) did not, while 22 (14.8%) were severe (categories 6 to 9) at the time of sampling. The mean age was 64.4 years, 65 (43.9%) were assigned female at birth, 38 (25.7%) had diabetes, 27 pre-existing lung disease (18.2%), 23 (15.5%) heart disease and 19 (12.8%) chronic renal failure. Patients' characteristics and comorbidities between moderate without progression, moderate with progression and severe disease status were similar, except for severe subjects being older (mean ages 64 vs. 73 years). The mean time from symptoms onset to hospital admission was seven days and most patients presented with cough (70.9%), dyspnoea (48%), diarrhoea (33.8%), and cephalgia (17.6%). Routine blood test results at the time of sampling showed significant differences between moderate patients without progression and those with progression to severity. Higher glucose and C-reactive protein levels and lower lymphocyte counts were observed in the patients who later progressed to severity. Patients who were already severe at baseline had even higher levels of glucose and C-reactive protein and presented an increased neutrophil count. Treatments included corticosteroids (87.2%), remdesivir (37.8%) and tocilizumab (30.4%). The median length of hospitalization stay was eight days, but was significantly longer in severe patients (7 vs 21.8). Twenty-six patients (17.6%) required a non-rebreather mask (NRB), 40 (27%) high flow nasal cannula (HFNC), two (1.4%) non-invasive (NIV) and eight (5.4%) invasive mechanical ventilation at any given time during hospitalization for at least 24h. Eleven (7.4%) patients were admitted to the intensive care unit (ICU), and in-hospital mortality was 6.8%.

### Metabolomic profile of severe COVID-19

In order to develop a metabolomic profile of severe COVID-19, the serum metabolites of patients with severe disease status (WHO Clinical Progression Scale categories 6–9) at the moment of sampling (n=22) were compared to those in patients with moderate disease status (WHO Clinical Progression Scale categories 4 or 5). Regarding the lipoprotein and glycoprotein analysis (Table 3), all lipid-related parameters (cholesterol and triglycerides) were significantly increased in severe disease status, except for HDL-C, which was reduced, and LDL-C, for which no differences were detected. Different lipoprotein particle concentrations were found, with an increase in total VLDL in severe patients driven by an increase of small VLDL particles; however, this did not lead to significant differences in the average size of VLDL particles. In contrast, severe disease status was associated with lower levels of small HDL particles and enlarged HDL particles. While no statistically significant differences in the particle concentration of LDL subclasses were found, mean LDL particle size was higher in severe patients. In addition, four out of the five glycoproteins analysed (Glyc-B, Glyc-A, H/W glyc-B, H/W Glyc-A) showed increased concentrations in severe patients. As for the analysis of low-molecular weight metabolites (Table 4), 3-hydroxybutyrate, glucose, glycerol, lactate, threonine, valine, isoleucine, and leucine were significantly increased in severe patients, and several lipid-related parameters (Table 5) showed higher concentrations in the severe group. When the moderate group was restricted to patients without progression towards severity (n = 108), all the previous parameters were still significant except for VLDL-TG, PL and PUFA4, which, although showing a trend, were no longer statistically significant.

### Prediction of progression towards severity

With a view to developing a model predictive of progression towards severity, moderate patients at baseline (WHO Clinical Progression Scale categories 4 or 5) who did not progress towards severity (WHO Clinical Progression Scale categories 6 to 9) over the course of hospitalization (n=108) were compared with those who did progress to severity (n=19). The univariate analysis showed nine parameters with significant differences (small LDL-P, medium HDL-P, Glyc-B, alanine, glutamine, isoleucine, SFA, w6+w7, and ARA+EPA), see Tables 3, 4 and 5.

We developed a multivariate statistical model to create a metabolomic signature of progression towards severity. Metabolite ratios were incorporated into the model in order to increase the statistical power. The 20

	Total (n = 148)	Moderate at baseline without progression (n = 107)	Moderate at baseline with progression (n = 19)	Severe at baseline (n = 22)	P-value
Demographic and clinical characteristics					
Age (mean), years	67.5 (22.0)	64.0 (23.8)	73.0 (15.0)	73.0 (22.0)	0.0264
Sex assigned at birth, n (%) women	65 (43.9)	48 (44.9)	8 (42.1)	9 (40.9)	0.9302
Body mass index (BMI), kg . m <sup>-2</sup>	30.0 (6.8)	30.5 (6.7)	27.0 (4.7)	31.4 (7.8)	0.0184
Obesity ≥ class II (BMI>35), n (%) yes	45 (30.4)	30 (28.0)	3 (15.8)	12 (54.6)	0.0161
Influenza vaccine, n (%) yes	72 (48.7)	50 (46.7)	13 (68.4)	9 (40.9)	0.1605
Risk factors*, n (%) yes	100 (67.6)	69 (64.5)	12 (63.2)	19 (86.4)	0.1237
Diabetes, n (%) yes	38 (25.7)	27 (25.2)	5 (26.3)	6 (27.3)	0.9780
Pre-existing lung disease, n (%) yes	27 (18.2)	20 (18.7)	4 (21.1)	3 (13.6)	0.8073
Heart disease, n (%) yes	23 (15.5)	16 (15.0)	2 (10.5)	5 (22.7)	0.5332
Chronic renal failure, n (%) yes	19 (12.8)	12 (11.2)	2 (10.5)	5 (22.7)	0.3222
Stroke, n (%) yes	5 (3.4)	4 (3.7)	0 (0.0)	1 (4.6)	0.6708
Hepatopathy, n (%) yes	5 (3.4)	4 (3.7)	0 (0.0)	1 (4.6)	0.6708
Blood test results					
Glucose. mg/dL	117.0 (38.8)	114.0 (32.0)	123.0 (39.8)	137.0 (110.0)	0.0262
Leucocytes/μL	6800 (3350)	6700 (3350)	5600 (3175)	8650 (8200)	0.0054
Neutrophils/μL	4870 (3210)	4690 (2917)	4270 (3015)	7050 (6630)	0.0009
Lymphocytes/μL	1000 (720)	1060 (635)	780 (1192)	845 (670)	0.0358
Platelets/μL	206000 (92000)	201000 (99250)	196000 (101250)	231500 (77000)	0.1035
Creatinine. μmol/L	73.5 (37.0)	73.0 (28.8)	91.0 (35.0)	82.0 (60.0)	0.1932
Uric acid. mg/L	32.0 (33.0)	29.5 (25.0)	39.0 (18.0)	54.5 (46.0)	0.1000
C-reactive protein. mg/L	82.7 (94.2)	69.2 (75.2)	104.6 (81.6)	141.5 (121.3)	< 0.0001
Symptoms and vital constants					
Cough, n (%) yes	105 (70.9)	77 (72.0)	12 (63.2)	16 (72.7)	0.7238
Dyspnoea, n (%) yes	71 (48.0)	43 (40.2)	9 (47.4)	19 (86.4)	0.0004
Diarrhoea, n (%) yes	50 (33.8)	38 (35.5)	6 (31.6)	6 (27.3)	0.7403
Cephalaea, n (%) yes	26 (17.6)	18 (16.8)	5 (26.3)	3 (13.6)	0.5273
Odynophagia, n (%) yes	10 (6.8)	6 (5.6)	1 (5.3)	3 (13.6)	0.3783
Days from symptoms onset to hospital admission	7.0 (5.5)	7.0 (5.0)	6.0 (3.8)	6.5 (6.0)	0.2572
Oxygen saturation (SO <sub>2</sub> ) %	95.0 (3.0)	95.0 (2.8)	95.0 (3.5)	88.0 (7.0)	< 0.0001
Systolic blood pressure (SBP) mmHg	131.5 (26.0)	134.0 (28.0)	124.0 (29.8)	127.0 (15.0)	0.1944
Diastolic blood pressure (DBP) mmHg	77.0 (18.0)	77.5 (20.0)	76.0 (18.3)	72.5 (22.0)	0.5928
Temperature °C	36.6 (0.8)	36.6 (0.7)	36.5 (1.0)	36.6 (1.3)	0.5400
Cardiac frequency bpm	88.0 (24.0)	86 (21.5)	90.0 (26.8)	89.5 (32.0)	0.8899

**Table 1.** Demographic data, clinical characteristics, blood test results, symptoms of the cohort of COVID-19 patients at the time of sampling (<48 hours of hospital admission). \*Risk factors refers to any patients with diabetes, heart disease, pre-existing lung disease, stroke or chronic renal failure. Moderate disease status is defined as category 4 or 5, and severe disease status as categories 6–9 following the WHO clinical progression scale. The *P*-value corresponds to the result of the Chi-square test for the qualitative variables and the Kruskal Wallis test for the quantitative ones.

most important ratios, based on their individual ability to distinguish progression towards severity and on the *p*-values resulting from a *t*-test, were included in the data set to build and validate the multivariate model. Our multivariate model presented a cross-validated AUC of 0.82 and a predictive accuracy of 72% (Fig. 1) for progression towards severity (WHO Clinical Progression Scale categories 6 to 9) for hospitalised COVID-19 patients with moderate disease status (WHO Clinical Progression Scale categories 4 or 5). The two most important variables in our multivariate model were the small LDL-P/medium HDL-P and LDL-C/medium HDL-P ratios (Figs. 2 and 3). While in the first case the two constituents (i.e., small LDL-P and medium HDL-P) were significant in our univariate analysis, in the second case only medium HDL-P was significant as an individual marker, while LDL-C presented a trend towards significance.

The 25 most important variables in our multivariate predictive model are shown in Fig. 2. Eighteen of them were metabolite ratios (and half of them had medium HDL-P as constituent). Furthermore, seven important ratios had one of the two constituents that, individually, were not discriminant of disease progression (univariate *P*-value > 0.1); these constituents were HDL-TG, large HDL-P, LDL-Z, leucine, glycerol, creatine, and SM.

	Total (n = 148)	Moderate without progression (n = 107)	Moderate with progression (n = 19)	Severe (n = 22)	P-value
COVID-19 treatments					
Corticosteroid, n (%) yes	129 (87.2)	88 (82.2)	19 (100.0)	22 (100.0)	0.0154
Remdesivir, n (%) yes	56 (37.8)	39 (36.4)	13 (68.4)	4 (18.2)	0.0036
Tocilizumab, n (%) yes	45 (30.4)	21 (19.6)	11 (57.9)	13 (59.1)	< 0.0001
Outcomes					
Median length of hospital stay (days, SD)	8.0 (7.0)	7.0 (4.0)	15.0 (10.8)	17.5 (16.0)	< 0.0001
NRB >24 h at any given time, n (%) yes	26 (17.6)	0 (0.0)	12 (63.2)	14 (63.6)	< 0.0001
HFNC >24h at any given time, n (%) yes	40 (27.0)	0 (0.0)	19 (100.0)	21 (95.5)	< 0.0001
NIV >24h at any given time, n (%) yes	2 (1.4)	0 (0.0)	1 (5.3)	1 (4.6)	0.0696
Invasive mechanical ventilation, n (%) yes	8 (5.4)	0 (0.0)	1 (5.3)	7 (31.8)	< 0.0001
Intensive care Unit admission, n (%) yes	11 (7.4)	1 (0.9)	2 (10.5)	8 (36.4)	< 0.0001
In-hospital mortality, n (%) yes	10 (6.8)	0 (0.0)	3 (15.8)	7 (31.8)	< 0.0001

**Table 2.** COVID-19 treatment and outcomes. NRB: non-rebreather mask; HFNC: high flow nasal cannula; NIV: non-invasive mechanical ventilation. Moderate disease status is defined as category 4 or 5, and severe disease status as categories 6–9 following the WHO clinical progression scale. The *P*-value corresponds to the result of the Chi-square test.

## Discussion

Our prospective study using an NMR-based analytical platform revealed a metabolomic profile indicative of severe COVID-19. We also identified a metabolomic signature capable of predicting progression towards severity at the time of hospital admission, preceding the onset of severe disease status.

Our metabolic profile associated with severe COVID-19 is broadly consistent with previous studies on metabolomics. We found profound changes in lipoprotein distribution in severe COVID-19 indicative of increased atherogenic risk; with an increase in small VLDL particles while small HDL particles numbers were lower. Small HDL particles, the HDL subspecies that presented the greatest reduction both in this study and in a previous study<sup>32</sup>, is also the HDL subspecies most strongly associated with cholesterol efflux capacity<sup>33</sup>. Severe disease status (WHO Clinical Progression Scale categories 6 to 9) was associated with an intense lipoprotein dysregulation towards increased TG, free cholesterol and anomalous lipoprotein distribution with elevated IDL-C, LDL-C and VLDL subclasses while HDL-C was reduced.

Our results are in line with those of previous studies which found a correlation between COVID-19 severity and high triglyceride concentrations, no-HDL-C and low plasma HDL-cholesterol<sup>14,34</sup>, an increased mean size of VLCL particles<sup>17</sup> and higher levels of free cholesterol<sup>14</sup>. As is to be expected, we also found elevated glyc-A and glyc-B signal in more severe patients. Glyc-A and glyc-B represent different glycosylated amino sugar residues on acute phase reactants<sup>35</sup>, with  $\alpha$ -1-acid glycoprotein having the strongest correlation with Glyc-A<sup>36</sup>. Previous studies have related glyc-A with chronic inflammation<sup>37</sup>, metabolic syndrome<sup>38</sup>, increased severity<sup>39,40</sup> and higher levels of CPR and IL-6 in COVID-19<sup>40</sup>. Furthermore, severe COVID-19 patients had elevated levels of branched-chained amino acids (BCAAs: leucine, isoleucine and valine) compared to their moderate COVID-19 peers, results which are concordant with prior studies<sup>16,21,41,42</sup>. BCAAs are essential amino acids which act as substrates and regulators of protein and glycogen metabolism<sup>43,44</sup>, and also modulate glucose metabolism. Elevated circulating levels of BCAAs are associated with catabolic states<sup>45</sup>, and, through mTOR activation, are linked to reactive oxygen species production and mitochondrial dysfunction<sup>46</sup> as well as to promoting endothelial dysfunction<sup>47</sup>. In addition, in accordance with prior studies, we found elevated glucose<sup>14</sup> and accumulation of ketone bodies in severe COVID-19 patients<sup>21,48</sup>, reflecting dysregulation of the hepatic carbon metabolism<sup>17</sup>.

When comparing moderate COVID-19 patients who did not progress to severity with those who did, several of the alterations in serum metabolites associated with severe disease status lost their significance. Most notably, no differences were found in free cholesterol, phospholipids, IDL, VLDL, HDL, suggesting that most of the intense lipoprotein dysregulation occurs at later stages of the disease. Higher levels of small LDL particles and a reduction in medium HDL particles, not present in the metabolomic comparison of moderate versus severe patients, were found to be predictive. A reduction of HDL has previously been associated with worse outcomes<sup>18,34</sup> and a predominance of small LDL particles compared to larger LDL particles has been identified in COVID-19 patients<sup>32</sup>. Increased levels of isoleucine, saturated fatty acids, and glyc-B, both associated with severe disease status, were also found to be predictive of progression to severity. Furthermore, our results indicated a higher risk of progression in patients with increased alanine and glutamine levels. These particular findings are surprising, as glutamine is essential for lymphocyte proliferation, cytokine production and macrophage activation, with increased demand in catabolic/hypercatabolic situations<sup>49</sup>. In addition, prior studies comparing uninfected controls versus COVID-19 patients found decreased levels of alanine<sup>41,50</sup> and glutamine<sup>17,39,51</sup>, as did another study of COVID-19 patients and severe COVID-19<sup>21</sup>. These diverging results may stem from differences in the cohorts under comparison. Patients with SARS-CoV-2 infection present lower glutamine levels than uninfected individuals; however, we compared moderate COVID-19 patients without progression with those who progressed at later stages. We also found higher levels of arachidonic acid in patients with progression.

Several strengths and limitations of our study should be acknowledged. First, we did not include COVID-19-negative controls, as the primary objective was to compare metabolic profiles within a cohort of COVID-19

Lipoproteins	Moderate at baseline (n = 22) vs severe at baseline (n = 127)			Moderate at baseline without progression (n = 108) vs severe at baseline (n = 22)			Moderate at baseline without progression (n = 19) vs moderate at baseline with progression (n = 108)		
	$\beta$	SE	P-value	$\beta$	SE	P-value	$\beta$	SE	P-value
VLDL-C	0.1037	0.0372	<b>0.0061</b>	0.1047	0.0387	<b>0.0078</b>	0.0315	0.1105	0.7762
IDL-C	0.1728	0.0349	<b>0.0000</b>	0.1721	0.0366	<b>0.0000</b>	0.0072	0.1075	0.9470
LDL-C	-0.0066	0.0177	0.7107	-0.0126	0.0182	0.4893	0.0982	0.0525	0.0643
HDL-C	-0.0417	0.0187	<b>0.0273</b>	-0.0394	0.0176	<b>0.0272</b>	-0.0536	0.0535	0.3186
VLDL-TG	0.0729	0.0349	<b>0.0386</b>	0.0698	0.0360	0.0551	0.1044	0.1018	0.3071
IDL-TG	0.1361	0.0266	<b>0.0000</b>	0.1378	0.0279	<b>0.0000</b>	-0.0031	0.0807	0.9699
LDL-TG	0.1233	0.0304	<b>0.0001</b>	0.1226	0.0317	<b>0.0002</b>	0.0433	0.0927	0.6413
HDL-TG	0.0710	0.0175	<b>0.0001</b>	0.0735	0.0183	<b>0.0001</b>	-0.0593	0.0544	0.2781
VLDL-P	0.0809	0.0344	<b>0.0203</b>	0.0792	0.0358	<b>0.0289</b>	0.0867	0.1005	0.3901
Large VLDL-P	0.0469	0.0263	0.0771	0.0450	0.0273	0.1029	0.0815	0.0758	0.2850
Medium VLDL-P	0.0664	0.0545	0.2253	0.0612	0.0554	0.2711	0.1310	0.1610	0.4176
Small VLDL-P	0.0823	0.0346	<b>0.0190</b>	0.0810	0.0361	<b>0.0266</b>	0.0864	0.1007	0.3929
LDL-P	0.0097	0.0172	0.5735	0.0042	0.0176	0.8138	0.0959	0.0506	0.0606
Large LDL-P	0.0147	0.0146	0.3140	0.0114	0.0151	0.4527	0.0467	0.0435	0.2856
Medium LDL-P	0.0517	0.0304	0.0916	0.0441	0.0314	0.1625	0.1394	0.0917	0.1312
Small LDL-P	-0.0119	0.0148	0.4237	-0.0169	0.0150	0.2630	0.0904	0.0432	<b>0.0384</b>
HDL-P	-0.0275	0.0163	0.0944	-0.0252	0.0155	0.1059	-0.0249	0.0469	0.5964
Large HDL-P	0.0129	0.0117	0.2721	0.0102	0.0114	0.3730	-0.0162	0.0347	0.6421
Medium HDL-P	0.0141	0.0124	0.2575	0.0169	0.0115	0.1452	-0.0863	0.0362	<b>0.0189</b>
Small HDL-P	-0.0573	0.0277	<b>0.0406</b>	-0.0586	0.0256	<b>0.0241</b>	0.0036	0.0822	0.9648
VLDL-Z	-0.0005	0.0006	0.3416	-0.0006	0.0006	0.2700	0.0001	0.0016	0.9353
LDL-Z	0.0023	0.0009	<b>0.0083</b>	0.0023	0.0009	<b>0.0083</b>	-0.0014	0.0025	0.5833
HDL-Z	0.0040	0.0013	<b>0.0030</b>	0.0040	0.0012	<b>0.0012</b>	-0.0061	0.0035	0.0903
Glycoproteins									
Glyc-B	0.0359	0.0127	<b>0.0054</b>	0.0353	0.0117	<b>0.0031</b>	0.0844	0.0375	<b>0.0264</b>
Glyc-F	0.0204	0.0147	0.1663	0.0198	0.0147	0.1788	0.0145	0.0458	0.7525
Glyc-A	0.0461	0.0146	<b>0.0020</b>	0.0452	0.0142	<b>0.0018</b>	0.0824	0.0438	0.0627
H/W Glyc-B	0.0351	0.0122	<b>0.0046</b>	0.0353	0.0119	<b>0.0037</b>	0.0473	0.0364	0.1963
H/W Glyc-A	0.0448	0.0133	<b>0.0010</b>	0.0452	0.0131	<b>0.0008</b>	0.0434	0.0405	0.2862

**Table 3.** Lipoproteins and glycoproteins comparison between groups. Analysis adjusted for body mass index, sex, smoking status, statins use and diabetes mellitus treatment of lipoprotein and glycoprotein in patients with severe versus moderate disease status at baseline, severe disease status at baseline versus moderate without progression to severity and moderate patients with progression versus moderate without progression. Significant *p* values are highlighted in bold. Moderate disease status is defined as category 4 or 5, and severe disease status as categories 6–9 following the WHO clinical progression scale. Abbreviations:  $\beta$  (regression coefficient), SE (standard error), VLDL-C (very-low-density lipoprotein cholesterol), IDL-C (intermediate-density lipoprotein cholesterol), HDL-C (high-density lipoprotein cholesterol), VLDL-TG (very-low-density lipoprotein triglycerides), IDL-TG (intermediate-density lipoprotein triglycerides), LDL-TG (low-density lipoprotein triglycerides), HDL-TG (high-density lipoprotein triglycerides), VLDL-P (very-low-density lipoprotein particle), LDL-P (low-density lipoprotein particle), HDL-P (high-density lipoprotein particle), VLDL-Z (very-low-density lipoprotein diameter), LDL-Z (low-density lipoprotein diameter), HDL-Z (high-density lipoprotein diameter).

patients, stratified by disease severity, rather than to examine differences between infected and uninfected individuals. This approach enhances the specificity of our metabolomic signature for predicting COVID-19 progression but limits conclusions about its distinction from similar profiles in other respiratory infections. Second, due to the nascent stage of vaccination within the general population in Spain at the time of the study, only unvaccinated patients without prior known SARS-CoV-2 exposure were included. Third, the study period coincided with the predominance of the Alpha (B.1.1.7) variant of SARS-CoV-2. Subsequent variants and subvariants might have elicited different host responses. Lastly, the sample size was relatively small – 148 patients, of whom 19 progressed following baseline sampling. However, the patients included in our study were followed up daily, which allowed an accurate assessment of their clinical course. Additionally, NMR spectroscopy-based metabolomic profiling allows for a rapid, highly accurate, non-destructive, and quantitative analysis. Unlike many studies that have used heterogeneous definitions of COVID-19 severity, potentially leading to misclassification due to the strain on healthcare resources recorded during surges, we defined severity according to the categories



	Severe at baseline (n = 22) vs moderate at baseline (n = 127)			Severe at baseline (n = 22) vs moderate at baseline without progression (n = 108)			Moderate at baseline with progression (n = 19) vs moderate at baseline without progression (n = 108)		
	$\beta$	SE	P-value	$\beta$	SE	P-value	$\beta$	SE	P-value
3-Hydroxybutyrate	0.3587	0.0939	<b>0.0002</b>	0.3739	0.0960	<b>0.0002</b>	-0.4490	0.2899	0.1244
Acetone	0.1119	0.0620	0.0733	0.1179	0.0632	0.0645	-0.1882	0.1845	0.3100
Alanine	-0.0294	0.0235	0.2136	-0.0367	0.0241	0.1297	0.1475	0.0729	<b>0.0456</b>
Creatinine	0.0071	0.0353	0.8406	0.0128	0.0362	0.7244	-0.0698	0.1056	0.5098
Creatine	0.0411	0.0332	0.2180	0.0394	0.0345	0.2559	0.1207	0.1016	0.2374
Glucose	0.1360	0.0324	<b>0.0001</b>	0.1403	0.0347	<b>0.0001</b>	0.0180	0.0998	0.8568
Glutamate	0.0658	0.0345	0.0589	0.0613	0.0344	0.0776	0.0465	0.1066	0.6635
Glutamine	-0.0195	0.0197	0.3257	-0.0274	0.0195	0.1620	0.1800	0.0591	<b>0.0029</b>
Glycerol	0.1357	0.0249	<b>0.0000</b>	0.1424	0.0260	<b>0.0000</b>	-0.0244	0.0761	0.7495
Glycine	0.0088	0.0240	0.7152	0.0072	0.0247	0.7702	0.0438	0.0676	0.5188
Histidine	-0.0010	0.0180	0.9569	-0.0010	0.0172	0.9554	0.0564	0.0545	0.3031
Lactate	0.1473	0.0294	<b>0.0000</b>	0.1505	0.0312	<b>0.0000</b>	-0.0865	0.0891	0.3341
Threonine	0.0582	0.0190	<b>0.0027</b>	0.0578	0.0202	<b>0.0050</b>	-0.0189	0.0546	0.7293
Tyrosine	-0.0086	0.0229	0.7090	-0.0098	0.0230	0.6696	0.0003	0.0721	0.9967
Valine	0.0568	0.0177	<b>0.0017</b>	0.0528	0.0188	<b>0.0059</b>	0.0439	0.0510	0.3911
Isoleucine	0.0842	0.0308	<b>0.0071</b>	0.0698	0.0315	<b>0.0288</b>	0.2134	0.0895	<b>0.0189</b>
Leucine	0.0912	0.0232	<b>0.0001</b>	0.0909	0.0244	<b>0.0003</b>	-0.0164	0.0684	0.8111

**Table 4.** Low-molecular-weight metabolites comparison between groups. Analysis adjusted for body mass index, sex, smoking status, statins use and diabetes mellitus treatment of low-molecular-weight metabolites (LMWM) in patients with severe versus moderate disease status at baseline, severe disease status at baseline versus moderate without progression to severity and moderate patients with progression versus moderate without progression. Significant *p* values are highlighted in bold. Moderate disease status is defined as category 4 or 5, and severe disease status as categories 6–9 following the WHO clinical progression scale. Abbreviations:  $\beta$  (regression coefficient), SE (standard error).

of the WHO Clinical Progression Scale. In contrast to several prior predictive metabolomic models, which often compare patients who already present severe disease with mild to moderate COVID-19 patients,<sup>13,22,25,26</sup> our approach involved comparing patients with equivalent clinical status at baseline. Furthermore, our multivariate model, incorporating metabolite ratios, showed a cross-validated AUC of 0.82 and a predictive accuracy of 72% for progression towards severity upon admission for hospitalised COVID-19 patients with moderate disease status and similar oxygen saturation.

In conclusion, severe COVID-19 was associated with a distinct metabolomic signature associated with an increased atherogenic risk and a pro-inflammatory catabolic state with dysregulated carbon metabolism. Notably, patients presenting with moderate disease but at a high risk of deterioration exhibit a characteristic metabolomic signature, which can be swiftly determined using NMR-based platforms, thereby providing a better metric for resource allocation and early treatment. These results should be assessed in larger prospective cohorts with other variants and in populations with pre-existing immunity. Moreover, our findings open up avenues for further research.

## Materials and methods

### Study subjects

In this prospective study, 148 patients were recruited at Bellvitge University Hospital. Metabolomic analyses were performed at Biosfer Teslab (Reus, Spain). Adult patients with a positive RT-PCR SARS-CoV-2 nasopharyngeal swab and COVID-19 hospitalised from January 2021 to May 2021 were eligible for inclusion. Recruitment and blood sampling was performed within 48h of hospital admission. We assigned patients a unique patient identifier (PID), which was then applied to the clinical samples and the de-identified data set. The list correlating the PID with the patient's identity was securely stored at Bellvitge University Hospital. The investigators followed up the patients prospectively and visited them until hospital discharge. Data on demographic and clinical characteristics, blood analysis, treatments, and outcomes were recorded.

To investigate metabolomic markers predictive of severe COVID-19 progression, we restricted our cohort to SARS-CoV-2-positive patients, stratified by clinical severity. The exclusion of COVID-19-negative controls allowed for a more focused analysis on identifying metabolic pathways and biomarkers specifically associated with disease progression among infected individuals. We compared the metabolomic profiles of patients with severe versus moderate COVID-19 at the time of sampling and with those of the subgroup of patients who remained moderate over the course of hospitalization. For the development of a signature predictive of progression towards severe disease status, we compared metabolomic profiles in moderate patients at the time of sampling who did not progress and in those who progressed to severity.

	Severe at baseline (n = 22) vs moderate at baseline (n = 127)			Severe at baseline (n = 22) vs moderate at baseline without progression (n = 108)			Moderate at baseline with progression (n = 19) vs moderate at baseline without progression (n = 108)		
	$\beta$	SE	P-value	$\beta$	SE	P-value	$\beta$	SE	P-value
EC	0.0160	0.0155	0.3027	0.0116	0.0156	0.4600	0.0771	0.0462	0.0983
FC	0.0376	0.0142	<b>0.0089</b>	0.0366	0.0148	<b>0.0145</b>	0.0178	0.0429	0.6786
TG	0.0893	0.0364	<b>0.0154</b>	0.0833	0.0378	<b>0.0296</b>	0.1307	0.1063	0.2216
PL	0.0341	0.0159	<b>0.0334</b>	0.0311	0.0167	0.0652	0.0525	0.0472	0.2683
PC	0.0401	0.0160	<b>0.0135</b>	0.0359	0.0167	<b>0.0337</b>	0.0666	0.0479	0.1671
SM	0.0032	0.0134	0.8104	0.0016	0.0137	0.9094	0.0331	0.0398	0.4068
LPC	0.0094	0.0242	0.6981	− 0.0003	0.0244	0.9892	0.1296	0.0719	0.0741
PUFA1	− 0.0155	0.0293	0.5982	− 0.0188	0.0294	0.5246	0.0754	0.0896	0.4021
PUFA2	0.0323	0.0352	0.3604	0.0225	0.0322	0.4873	0.2185	0.1110	0.0515
PUFA3	− 0.0062	0.0226	0.7852	− 0.0085	0.0232	0.7155	0.0596	0.0664	0.3712
PUFA4	0.0539	0.0270	<b>0.0480</b>	0.0482	0.0282	0.0905	0.1433	0.0814	0.0811
Linoleic	0.0476	0.0281	0.0922	0.0397	0.0265	0.1371	0.1665	0.0868	0.0577
SFA	0.0503	0.0187	<b>0.0080</b>	0.0396	0.0184	<b>0.0331</b>	0.1322	0.0560	<b>0.0200</b>
w6+w7	0.0476	0.0184	<b>0.0108</b>	0.0407	0.0186	<b>0.0306</b>	0.1168	0.0550	<b>0.0360</b>
w9	0.0890	0.0353	<b>0.0129</b>	0.0933	0.0369	<b>0.0128</b>	− 0.0187	0.1069	0.8616
w3	0.0266	0.0237	0.2639	0.0282	0.0250	0.2623	0.0436	0.0704	0.5376
DHA	0.0405	0.0310	0.1939	0.0332	0.0324	0.3081	0.1370	0.0951	0.1529
ARA+EPA	− 0.0134	0.0204	0.5109	− 0.0184	0.0201	0.3615	0.1181	0.0593	<b>0.0490</b>

**Table 5.** Lipids comparison between groups. Analysis adjusted for body mass index, sex, smoking status, statins use and diabetes mellitus treatment of lipids in patients with severe versus moderate disease status at baseline, severe disease status at baseline versus moderate without progression to severity and moderate patients with progression versus moderate without progression. Significant *p* values are highlighted in bold. Moderate disease status is defined as category 4 or 5, and severe disease status as categories 6–9 following the WHO clinical progression scale. Abbreviations:  $\beta$  (regression coefficient), SE (standard error), EC (esterified cholesterol), FC (free cholesterol), TG (triglycerides), PL (phospholipids), PC (phosphatidylcholine), SM (sphingomyelin), LPC (Lysophosphatidylcholine), PUFA (polyunsaturated fatty acids), SFA (saturated fatty acids), DHA (Docosahexaenoic acid). ARA (Arachidonic Acid), EPA (eicosapentaenoic acid).

Definitions and local guidelines

COVID-19 pneumonia was defined as new or worsening pulmonary infiltrates on a chest x-ray or CT of the lungs with a confirmed positive RT-PCR for SARS-CoV-2. Severity was defined according to the patient’s respiratory situation and using the WHO Clinical Progression Scale<sup>52</sup>. In brief, moderate disease comprises categories 4 (hospitalised with no oxygen therapy) and 5 (hospitalised with oxygen by mask or nasal prongs) while severe disease includes categories 6–9 (referring to patients requiring high-flow oxygen and non-invasive or invasive mechanical ventilation with varying degrees of organ failure). Institutional guidelines at the moment of study recommended corticosteroids, preferably dexamethasone at a daily dose of 6mg, for all patients >7 days from symptoms onset and requiring oxygen supplementation. Tocilizumab was recommended for patients with C-reactive protein >75 mg/dl and severe disease status and/or progression towards severity. Remdesivir was recommended for patients with low-flow oxygen requirement (oxygen mask or nasal prongs) and <7 days from symptoms onset.

Metabolomics analyses

Lipoprotein profile

The lipoprotein profile was measured in serum samples (250  $\mu$ L) using the <sup>1</sup>H-NMR-based Liposcale test, a new generation nuclear magnetic resonance test by Biosfer Teslab (Reus, Spain). The lipid concentrations (i.e., triglycerides and cholesterol) of the four main classes of lipoproteins (very low-density lipoprotein (VLDL); intermediate-density lipoprotein (IDL), low-density lipoprotein (LDL), and high-density lipoprotein (HDL)), and the particle numbers of nine subclasses (large, medium, and small particle numbers of each of the following: VLDL, LDL, and HDL) were determined as previously reported<sup>53</sup>. The different lipoprotein subclasses corresponded to the following diameter size ranges: large VLDL, 68.5–95.9 nm; medium VLDL, 47–68.5 nm; small VLDL, 32.5–47 nm; large LDL, 24–32.5 nm; medium LDL, 20.5–24 nm; small LDL, 17.5–20.5 nm; large HDL, 10.5–13.5 nm; medium HDL, 8.5–10.5 nm; and small HDL, 7.5–8.5 nm.

Glycoprotein profile

The glycoprotein profile was determined by analysing the specific <sup>1</sup>H-NMR spectral region where these protein–sugar bonds resonate (2.15–1.90 ppm) by deconvoluting the spectra by using three Lorentzian functions, as

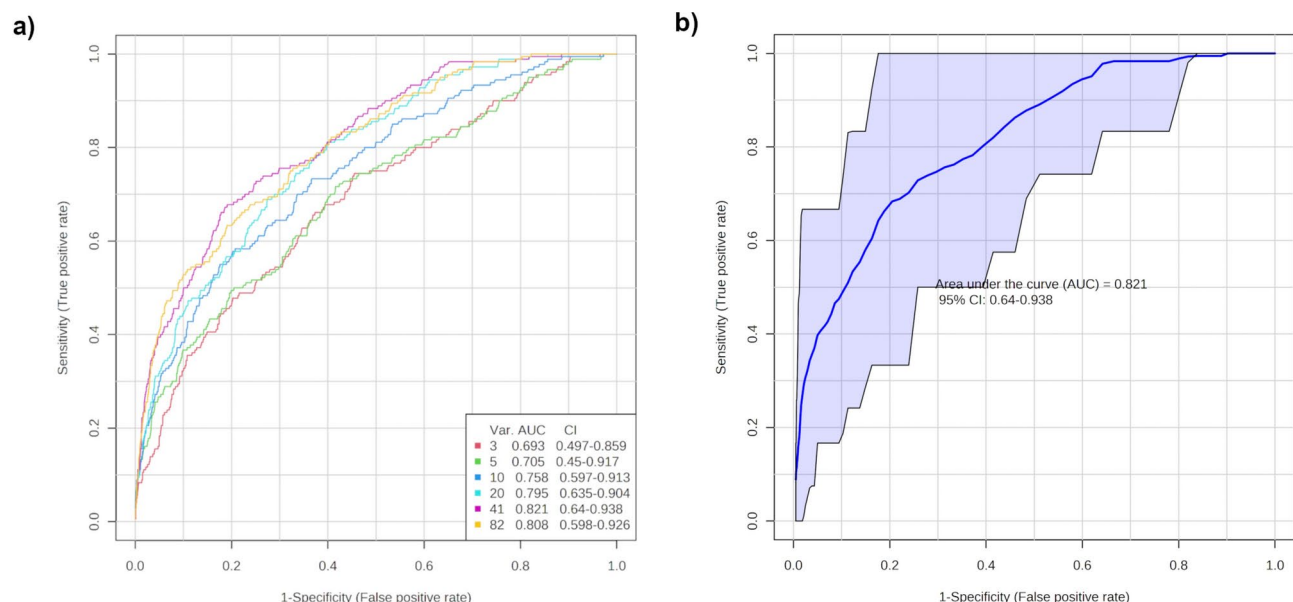


**Fig. 1.** Area under the curve (AUC) of the sensitivity (a) and specificity (b) of the multivariate model for progression towards severity (WHO clinical progression scale categories 6–9) for hospitalised COVID-19 patients with moderate disease status (WHO clinical progression scale categories 4 or 5). The model shows a predictive accuracy of 72% with a cross-validated AUC of 0.82.

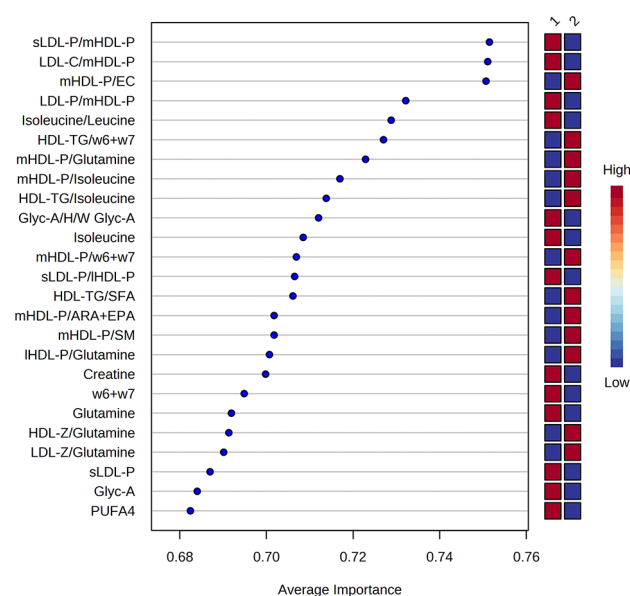


**Fig. 2.** The 25 most important variables for predicting progression towards severity (WHO clinical progression scale categories 6–9) for hospitalised COVID-19 patients with moderate disease status (WHO clinical progression scale categories 4 or 5). Eighteen of them are metabolite ratios included in the data set to build and validate the multivariate predictive model. Class 1: moderate disease status with progression; Class 2: moderate disease status without progression.

previously reported<sup>54</sup>. For each function, we determined the total area (proportional to concentration), height, position, and bandwidth. The area of glycoprotein A (Glyc-A) provided the concentration of acetyl groups of protein-bound N-acetylglucosamine and N-acetylgalactosamine, and the area of glycoprotein B (Glyc-B) provided the concentration of N-acetylneuraminic acid. The glycoprotein F (Glyc-F) area arises from the concentration in the acetyl groups of N-acetylglucosamine, N-acetylgalactosamine, and N-acetylneuraminic acid unbound to proteins (free fraction). H/W ratios, which reflect the aggregation state of the sugar-protein bonds, were also reported for Glyc-A and Glyc-B<sup>55</sup>. Height was calculated as the difference from the baseline to maximum of the corresponding NMR peaks, and the width value corresponded to the peak width at half height.



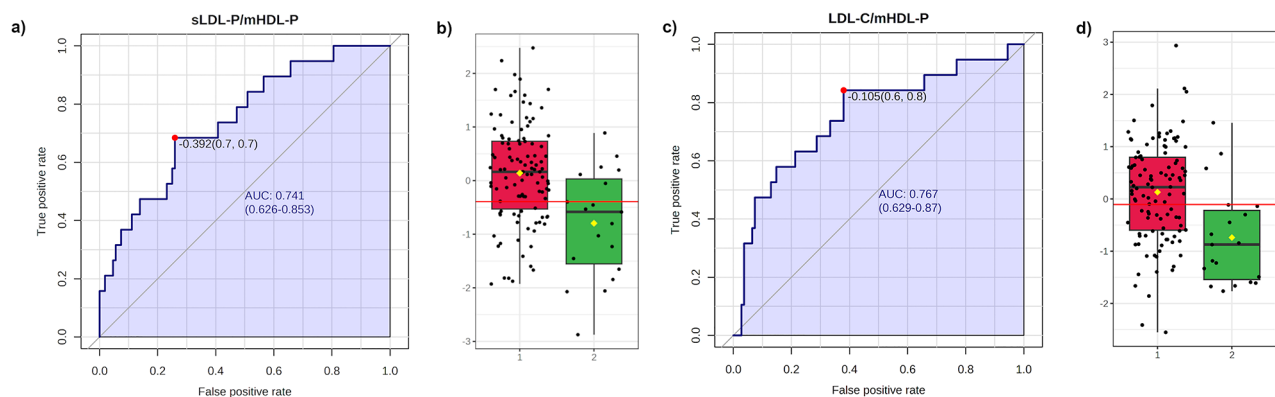


**Fig. 3.** Individual ability to distinguish progression towards severity (WHO Clinical Progression Scale categories 6–9) for hospitalised COVID-19 patients with moderate disease status (WHO Clinical Progression Scale categories 4 or 5) according to the two most important variables of our multivariate model: small LDL-P/medium HDL-P (a and b) and LDL-C/medium HDL-P ratios (c and d). Class 1: moderate disease status with progression; Class 2: moderate disease status without progression.

#### Low molecular weight metabolites (LMWMs) profile

Intact serum was analysed by  $^1\text{H}$ -NMR using a one-dimensional Carr-Purcell-Meiboom-Gill (CPMG) pulse. LMWMs were identified using an adaptation of Dolphin<sup>56</sup>. Each metabolite was identified by checking for all its resonances along the spectra and then quantified using line-shape fitting methods on one of its signals.

#### Lipidomic profile

Lipophilic extracts were obtained from two 100  $\mu\text{L}$  aliquots of freshly thawed plasma using the BUME method<sup>56</sup> with slight modifications. Specifically, BUME was optimized for batch extractions with di-isopropyl ether (DIPE) replacing heptane as the organic solvent. This procedure was performed with a BRAVO liquid handling robot, which has the capacity to extract 96 samples at once. The upper lipophilic phase was completely dried in Speedvac until evaporation of organic solvents and frozen at  $-80^\circ\text{C}$  until NMR analysis. Lipid extracts were reconstituted in a solution of  $\text{CDCl}_3:\text{CD}_3\text{OD}:\text{D}_2\text{O}$  (16:7:1, v/v/v) containing tetramethylsilane (TMS) at 1.18 mM as a chemical shift reference and transferred into 5-mm NMR glass tubes.  $^1\text{H}$ -NMR spectra were measured at 600.20 MHz using an Avance III 600 Bruker spectrometer. A  $90^\circ$  pulse with water pre-saturation sequence (zgpr) was used. Quantification of lipid signals in  $^1\text{H}$ -NMR spectra was carried out with LipSpin<sup>57</sup>. Resonance assignments were made based on values in the literature<sup>58</sup>.

#### Statistical analysis

##### General data analysis procedures

Except when otherwise stated, all data are presented as the mean and interquartile range (IQR) for continuous variables. Differences in the mean values of clinical variables across groups were assessed using the Kruskal Wallis test for continuous variables and the Chi-square test for categorical variables. Negative and zero values in the metabolomics data set were set to “not a number”. The association between disease status (exposure) and log-transformed metabolomics profiles (outcome) was assessed using linear regression models adjusted by body mass index (BMI), sex, smoking status, statins use, and presence of diabetes treatment. Finally, the diagnostic performance of the metabolomics profiles was assessed by means of the MetaboAnalyst platform<sup>59</sup>. First, the metabolomics data set was normalized by median and scaled using the autoscale scaling method. Then, a partial least squares-discriminant analysis (PLS-DA) multivariate model with two latent variables provided in this platform was used to build a predictive model, where features were ranked according to its individual diagnostic performance based on area under the curve (AUC) score. Also, our multivariate analysis included metabolite ratios (top 20 metabolite ratios based on individual performance). Finally, ROC curves were generated by Monte-Carlo cross validation (MCCV) using balanced sub-sampling. In brief, in each MCCV, two-thirds (2/3) of the samples were used to evaluate the feature importance. The top 3, 5, 10, 20, 50, and 100 important features were then used to build classification models which were validated on the third of the samples that were left out. The procedure was repeated multiple times to calculate the performance and confidence interval of each model.

#### Data availability

The raw data generated in this study is publicly available on Zenodo, a general-purpose open-access repository, and can be accessed via the following link: <https://doi.org/10.5281/zenodo.14687731>.

Received: 7 April 2024; Accepted: 17 January 2025

Published online: 10 February 2025

#### References

1. Gandhi, R. T., Lynch, J. B. & del Rio, C. Mild or moderate Covid-19. *N. Engl. J. Med.* **383**, 1757–1766 (2020).

2. Berlin, D. A., Gulick, R. M. & Martinez, F. J. Severe Covid-19. *N. Engl. J. Med.* **383**, 2451–2460 (2020).
3. Ellinghaus, D. et al. Genomewide association study of severe Covid-19 with respiratory failure. *N. Engl. J. Med.* **383**, 1522–1534 (2020).
4. Suryamohan, K. et al. Human ACE2 receptor polymorphisms and altered susceptibility to SARS-CoV-2. *Commun. Biol.* **4**, 475 (2021).
5. Aydiello, T. et al. Immunological imprinting of the antibody response in COVID-19 patients. *Nat. Commun.* **12**, 3781 (2021).
6. Chan, Y. et al. Asymptomatic COVID-19: Disease tolerance with efficient anti-viral immunity against SARS-CoV-2. *EMBO Mol. Med.* **13**, 1–15 (2021).
7. Fang, F. C. et al. COVID-19-lessons learned and questions remaining. *Clin. Infect. Dis.* **72**, 2225–2240 (2021).
8. Rombauts, A. et al. Dynamics of gene expression profiling and identification of high-risk patients for severe COVID-19. *Biomedicine* **11**, 1348 (2023).
9. <https://www.cdc.gov/mmwr/volumes/71/wr/mm7137a4.htm>.
10. Berenguer, J. et al. Characteristics and predictors of death among 4035 consecutively hospitalized patients with COVID-19 in Spain. *Clin. Microbiol. Infect.* <https://doi.org/10.1016/j.cmi.2020.07.024> (2020).
11. Guan, W. et al. Clinical characteristics of coronavirus disease 2019 in China. *N. Engl. J. Med.* **382**, 1708–1720 (2020).
12. Delafiori, J. et al. Covid-19 automated diagnosis and risk assessment through metabolomics and machine learning. *Anal. Chem.* **93**, 2471–2479 (2021).
13. López-Hernández, Y. et al. Targeted metabolomics identifies high performing diagnostic and prognostic biomarkers for COVID-19. *Sci. Rep.* **11**, 14732 (2021).
14. Song, J. W. et al. Omics-driven systems interrogation of metabolic dysregulation in COVID-19 pathogenesis. *Cell Metab.* **32**, 188 (2020).
15. Wu, D. et al. Plasma metabolomic and lipidomic alterations associated with COVID-19. *Natl. Sci. Rev.* **7**, 113 (2020).
16. Sameh, M. et al. Integrated multiomics analysis to infer COVID-19 biological insights. *Sci. Rep.* **13**, 1802 (2023).
17. Bruzzzone, C. et al. SARS-CoV-2 infection dysregulates the metabolomic and lipidomic profiles of serum. *iScience* **23**, 101645 (2020).
18. Overmyer, K. A. et al. Large-scale multi-omic analysis of COVID-19 Severity. *Cell Syst.* **12**, 23 (2021).
19. Chen, Y. et al. Blood molecular markers associated with COVID-19 immunopathology and multi-organ damage. *EMBO J.* **39**, e105896 (2020).
20. Gardinassi, L. G. et al. Integrated metabolic and inflammatory signatures associated with severity of, fatality of, and recovery from COVID-19. *Microbiol. Spectr.* **11**, e02194–22 (2023).
21. Páez-Franco, J. C. et al. Metabolomics analysis reveals a modified amino acid metabolism that correlates with altered oxygen homeostasis in COVID-19 patients. *Sci. Rep.* **11**, 6350 (2021).
22. Soares, N. C. et al. Plasma metabolomics profiling identifies new predictive biomarkers for disease severity in COVID-19 patients. *PLoS One* **18**, 1–20 (2023).
23. Van Oostdam, A. S. H. et al. Immunometabolic signatures predict risk of progression to sepsis in COVID-19. *PLoS One* **16**, e0256784 (2021).
24. Caterino, M. et al. Dysregulation of lipid metabolism and pathological inflammation in patients with COVID-19. *Sci. Rep.* **11**, 2941 (2021).
25. D'Amora, P. et al. Towards risk stratification and prediction of disease severity and mortality in COVID-19: Next generation metabolomics for the measurement of host response to COVID-19 infection. *PLoS One* **16**, e0259909 (2021).
26. Sindelar, M. et al. Longitudinal metabolomics of human plasma reveals prognostic markers of COVID-19 disease severity. *Cell Rep. Med.* **2**, 100369 (2021).
27. Anson, L. et al. Amino acid metabolism is significantly altered at the time of admission in hospital for severe COVID-19 patients: Findings from longitudinal targeted metabolomics analysis. *Microbiol. Spectr.* **9**, e00338–21 (2021).
28. Chen, Y. et al. Blood molecular markers associated with COVID-19 immunopathology and multi-organ damage. *EMBO J.* **39**, e105896 (2020).
29. Beckonert, O. et al. Metabolic profiling, metabolomic and metabolomic procedures for NMR spectroscopy of urine, plasma, serum and tissue extracts. *Nat. Protoc.* **2**, 2692–2703 (2007).
30. Nicholson, J. K., Lindon, J. C. & Holmes, E. 'Metabonomics': Understanding the metabolic responses of living systems to pathophysiological stimuli via multivariate statistical analysis of biological NMR spectroscopic data. *Xenobiotica* **29**, 1181–1189 (1999).
31. Costantini, S. et al. New insights into the identification of metabolites and cytokines predictive of outcome for patients with severe SARS-CoV-2 infection showed similarity with cancer. *Int. J. Mol. Sci.* **24**, 4922 (2023).
32. Ballout, R. A. et al. The NIH lipo-COVID study: A pilot NMR investigation of lipoprotein subfractions and other metabolites in patients with severe COVID-19. *Biomedicine* **9**, 1090 (2021).
33. Heinecke, J. W. Small HDL promotes cholesterol efflux by the ABCA1 pathway in macrophages: Implications for therapies targeted to HDL. *Circ. Res.* **116**, 1101–1103 (2015).
34. Masana, L. et al. Low HDL and high triglycerides predict COVID-19 severity. *Sci. Rep.* **11**, 7217 (2021).
35. Holmes, E. et al. Diffusion and relaxation edited proton NMR spectroscopy of plasma reveals a high-fidelity supramolecular biomarker signature of SARS-CoV-2 infection. *Anal. Chem.* **93**, 3976–3986 (2021).
36. Otvos, J. D. et al. GlycA: A composite nuclear magnetic resonance biomarker of systemic inflammation. *Clin. Chem.* **61**, 714–723 (2015).
37. Ritchie, S. C. et al. The biomarker GlycA is associated with chronic inflammation and predicts long-term risk of severe infection. *Cell Syst.* **1**, 293–301 (2015).
38. Gruppen, E. G., Connelly, M. A., Otvos, J. D., Bakker, S. J. & Dullaart, R. P. A novel protein glycan biomarker and LCAT activity in metabolic syndrome. *Eur J Clin Invest.* **45**(8), 850–859. <https://doi.org/10.1111/eci.12481> (2015).
39. Ghini, V. et al. Profiling metabolites and lipoproteins in COMETA, an Italian cohort of COVID-19 patients. *PLoS Pathog.* **18**, e1010443 (2022).
40. Rössler, T. et al. Quantitative serum NMR spectroscopy stratifies COVID-19 patients and sheds light on interfaces of host metabolism and the immune response with cytokines and clinical parameters. *Metabolites* **12**, 1277 (2022).
41. Banach, M. et al. Association between circulating amino acids and COVID-19 severity. *Metabolites* <https://doi.org/10.3390/metab013020201> (2023).
42. Danlos, F. X. et al. Metabolomic analyses of COVID-19 patients unravel stage-dependent and prognostic biomarkers. *Cell Death Dis.* **12**, 258 (2021).
43. Holeček, M. The BCAA-BCKA cycle: Its relation to alanine and glutamine synthesis and protein balance. *Nutrition* **17**, 70 (2001).
44. Monirujjaman, M. & Ferdouse, A. Metabolic and physiological roles of branched-chain amino acids. *Adv. Mol. Biol.* **2014**, 1–6 (2014).
45. Holeček, M. Why are branched-chain amino acids increased in starvation and diabetes?. *Nutrients* **12**, 1–15 (2020).
46. Zhenyukh, O. et al. High concentration of branched-chain amino acids promotes oxidative stress, inflammation and migration of human peripheral blood mononuclear cells via mTORC1 activation. *Free Radic. Biol. Med.* **104**, 165–177 (2017).
47. Zhenyukh, O. et al. Branched-chain amino acids promote endothelial dysfunction through increased reactive oxygen species generation and inflammation. *J. Cell. Mol. Med.* **22**, 4948–4962 (2018).

48. Shi, D. et al. The serum metabolome of COVID-19 patients is distinctive and predictive. *Metabolism* **118**, 154739 (2021).
49. Cruzat, V., Rogero, M. M., Keane, K. N., Curi, R. & Newsholme, P. Glutamine: Metabolism and immune function, supplementation and clinical translation. *Nutrients* **10**, 1–31 (2018).
50. Caterino, M. et al. The serum metabolome of moderate and severe covid-19 patients reflects possible liver alterations involving carbon and nitrogen metabolism. *Int. J. Mol. Sci.* **22**, 1–18 (2021).
51. Masuda, R. et al. Integrative modeling of plasma metabolic and lipoprotein biomarkers of SARS-CoV-2 infection in Spanish and Australian COVID-19 patient cohorts. *J. Proteome Res.* **20**, 4139–4152 (2021).
52. Marshall, J. C. et al. A minimal common outcome measure set for COVID-19 clinical research. *Lancet. Infect. Dis.* **20**, e192–e197 (2020).
53. Mallol, R. et al. Liposcale: A novel advanced lipoprotein test based on 2D diffusion-ordered <sup>1</sup>H NMR spectroscopy. *J. Lipid Res.* **56**, 737–746 (2015).
54. Fuertes-Martín, R. et al. Characterization of <sup>1</sup>H NMR plasma glycoproteins as a new strategy to identify inflammatory patterns in rheumatoid arthritis. *J. Proteome Res.* **17**, 3730–3739 (2018).
55. Fuertes-Martín, R. et al. Glycoprotein A and B height-to-width ratios as obesity-independent novel biomarkers of low-grade chronic inflammation in women with polycystic ovary syndrome (PCOS). *J. Proteome Res.* **18**, 4038–4045 (2019).
56. Gómez, J. et al. Dolphin: A tool for automatic targeted metabolite profiling using 1D and 2D <sup>1</sup>H-NMR data. *Anal. Bioanal. Chem.* **406**, 7967–7976 (2014).
57. Barrilero, R. et al. LipSpin: A new bioinformatics tool for quantitative <sup>1</sup>H NMR lipid profiling. *Anal. Chem.* **90**, 2031–2040 (2018).
58. Löfgren, L. et al. The BUMe method: A novel automated chloroform-free 96-well total lipid extraction method for blood plasma. *J. Lipid Res.* **53**, 1690–1700 (2012).
59. <https://www.metaboanalyst.ca/>.

## Acknowledgements

A.R. received a predoctoral research grant from the Instituto de Salud Carlos III, the Spanish Ministry of Science, Innovation, and Universities, (PFIS grant FI18/00183). G.A.A. received a predoctoral research grant from the Instituto de Salud Carlos III, the Spanish Ministry of Science, Innovation, and Universities (CM21/00047), co-funded by European Social Fund (ESF) investing in your future. The project was supported through a grant from the Department de Salut of the Generalitat de Catalunya (20DPS005) and from the Instituto de Salud Carlos III, Madrid, Spain (COV20\_00121). We thank the CERCA Programme/Generalitat de Catalunya for their institutional support. The authors would like to thank all the members of the Clinical Research Support Unit (HUB-IDIBELL) for selflessly allowing the use of their facilities.

## Author contributions

Conceptualization, A.R., C.G., and J.C.; Sample acquisition and patient follow-up: A.R., G.A.; Data curation and formal analysis, R.M., M.B.; Funding acquisition, J.C.; Methodology, A.R., J.C., C.G., and R.M.; Project administration, J.C.; Supervision, C.G. and J.C.; Visualization, J.C.; Writing—original draft, A.R., R.M., and J.C.; Writing—review and editing, A.R., G.A., R.M., M.B., C.G., and J.C. All authors have read and agreed to the published version of the manuscript.

## Declarations

## Competing Interests

Roger Mallol owns stock in Biosfer Teslab. The rest of authors declare no competing interests.

## Ethical approval

The study was approved by the Bellvitge University Hospital Ethics Committee (PR037/21) in accordance with Spanish legislation, and the procedures followed complied with the ethical standards of the Helsinki Declaration. Written informed consent was obtained for all cases.

## Additional information

**Correspondence** and requests for materials should be addressed to A.R.

**Reprints and permissions information** is available at [www.nature.com/reprints](http://www.nature.com/reprints).

**Publisher's note** Springer Nature remains neutral with regard to jurisdictional claims in published maps and institutional affiliations.

**Open Access** This article is licensed under a Creative Commons Attribution-NonCommercial-NoDerivatives 4.0 International License, which permits any non-commercial use, sharing, distribution and reproduction in any medium or format, as long as you give appropriate credit to the original author(s) and the source, provide a link to the Creative Commons licence, and indicate if you modified the licensed material. You do not have permission under this licence to share adapted material derived from this article or parts of it. The images or other third party material in this article are included in the article's Creative Commons licence, unless indicated otherwise in a credit line to the material. If material is not included in the article's Creative Commons licence and your intended use is not permitted by statutory regulation or exceeds the permitted use, you will need to obtain permission directly from the copyright holder. To view a copy of this licence, visit <http://creativecommons.org/licenses/by-nc-nd/4.0/>.

© The Author(s) 2025